Bone Reports 5 (2016) 262–273

Contents lists available at ScienceDirect

Bone Reports

journal homepage: www.elsevier.com/locate/bonr

Effects of total flavonoids from Drynariae Rhizoma prevent bone loss in vivo and in vitro

Shuang-hong Song [a,b,d], Yuan-kun Zhai [c], Cui-qin Li [b,d], Qian Yu [b,d], Yi Lu [a], Yuan Zhang [b,d], Wen-ping Hua [b,d], Zhe-zhi Wang [b,d], Peng Shang [a,*]

[a] Key Laboratory for Space Bioscience and Biotechnology, Institute of Special Environmental Biophysics, School of Life Sciences, Northwestern Polytechnical University, Xi'an 710072, China
[b] Key Laboratory of the Ministry of Education for Medicinal Resources and Natural Pharmaceutical Chemistry, College of Life Sciences, Shaanxi Normal University, Xi'an 710062, China
[c] Department of Physiology and Biophysics, School of Medicine, University of Louisville, Louisville, KY 40202, USA
[d] National Engineering Laboratory for Resource Developing of Endangered Chinese Crude Drugs in Northwest of China, College of Life Sciences, Shaanxi Normal University, Xi'an 710062, China

ARTICLE INFO

Article history:
Received 27 July 2016
Received in revised form 2 September 2016
Accepted 9 September 2016
Available online 10 September 2016

Keywords:
Osteoporosis
Osteoblast
Osteoclast
Ovariectomy
Drynariae Rhizoma

ABSTRACT

Estrogen deficiency is one of the major causes of osteoporosis in postmenopausal women. Drynariae Rhizoma is a widely used traditional Chinese medicine for the treatment of bone diseases. In this study, we investigated the therapeutic effects of the total Drynariae Rhizoma flavonoids (DRTF) on estrogen deficiency-induced bone loss using an ovariectomized rat model and osteoblast-like MC3T3-E1 cells. Our results indicated that DRTF produced osteo-protective effects on the ovariectomized rats in terms of bone loss reduction, including decreased levels of bone turnover markers, enhanced biomechanical femur strength and trabecular bone microarchitecture deterioration prevention. In vitro experiments revealed that the actions of DRTF on regulating osteoblastic activities were mediated by the estrogen receptor (ER) dependent pathway. Our data also demonstrated that DRTF inhibited osteoclastogenesis via up-regulating osteoprotegrin (OPG), as well as down-regulating receptor activator of NF–κB ligand (RANKL) expression. In conclusion, this study indicated that DRTF treatment effectively suppressed bone mass loss in an ovariectomized rat model, and in vitro evidence suggested that the effects were exerted through actions on both osteoblasts and osteoclasts.

1. Introduction

As the population ages, osteoporosis is becoming an increasingly common disease. It is a major public health problem worldwide, which requires effective medicine or approaches for prevention and treatment (Banu et al., 2012). In particular, postmenopausal women are at high risk of developing osteoporosis due to significant alterations in bone metabolism associated with estrogen deficiency. The rapid bone loss and high bone fragility during menopause lead to increasing incidence rates of spine, hip and wrist fractures among postmenopausal women (Al-Anazi et al., 2011; Sundeep, 2010).Estrogen replacement therapy (ERT), which is the major therapy for the prevention and treatment of postmenopausal osteoporosis (PMOP) (Kyvernitakis et al., 2015), was reported to be associated with an increased risk of breast cancer, ovarian cancer, endometrial cancer and cardiovascular disease development in postmenopausal women (Davison and Davis, 2003; Foidart et al., 2007; Morch et al., 2009). Thus, development of affordable and alternative approaches with minimal side effects for PMOP has attracted a great deal of attention. This is particularly important for aging populations in developing countries, in which the majority of patients cannot afford the long-term use of high-cost medications. Recently, dietary phytoestrogens have been shown to be a rich source of plant-derived natural compounds and have been identified as safe and effective candidate drugs with estrogenic properties in the treatment of PMOP (Cassidy, 2003). Plenty of Chinese herbs that are traditionally used for the treatment of bone diseases exert estrogen-like activities on bone (Chen et al., 2011b; Zhang et al., 2010; Zhang et al., 2011) and might serve as a potential source of phytoestrogens for the management of PMOP. These phytoestrogens include soya isoflavones (Zhang et al., 2008; Zhang et al., 2009), lignans (Lampe, 2003), and flavonoids (Mok et al., 2010; Pang et al., 2010). Previous reports showed that phytoestrogens attenuated bone loss associated with estrogen deficiency in both animal and human studies (Dixon, 2004).

Drynariae Rhizoma is the dried rhizome of perennial pteridophyte *Drynaria fortunei* (Kunze) J. Sm. (Polypodiaceae). As a traditional Chinese medicine, Drynariae Rhizoma is widely used for the treatment of bone fractures or related diseases in Asian countries. In Chinese it is named "Gusuibu" which means bone fractures healer (Huang et al., 2014). The crude extract of Drynariae Rhizoma has been shown to promote osteoblast differentiation and mineralization in preosteoblastic cells (Chen et al., 2011a) as well as inhibit bone resorption in mouse osteoclasts in vitro (Jeong et al., 2003). In vivo research indicated that administration of Drynariae Rhizoma crude extract to 8-week-old BALB/c

* Corresponding author.
E-mail address: shangpeng@nwpu.edu.cn (P. Shang).

http://dx.doi.org/10.1016/j.bonr.2016.09.001

male mice for 5 weeks could increase bone density by 6.45% and the trabecular number by 10%. Additionally, Rhizoma Drynariae extracts can also induce bone formation on the margins of defects created in New Zealand white rabbits parietal bone (Wong et al., 2007).

The major bioactive constituents of Drynariae Rhizoma are flavonoids, which have attracted considerable attention for their potential roles in osteoporosis prevention and stimulatory activity on osteoblasts differentiation (Wang et al., 2008). Naringin and neoeriocitrin are the two major flavonoid compounds with the highest concentrations in Drynariae Rhizoma (Xu et al., 2016). It has been reported that naringin exerts positive effects in bone via ER-dependent pathways (Lu et al., 2006). Although these results are encouraging, whether DRTF exerts estrogen-like activities, has beneficial effects in estrogen deficiency-induced osteoporotic rats and the possible molecular mechanisms for this remain to be explained. To address these questions, the anti-osteoporotic effects and the potential mechanisms of DRTF on osteoporosis prevention and treatment were systematically investigated and 17-β-estradiol (E_2) was used as a positive control drug in the present study.

2. Materials and methods

2.1. Reagents

Total Drynariae Rhizoma flavonoids (DRTF) were purchased from Beijing Qihuang Pharmaceutical Manufacturing Co., Ltd. (National Medicine Permit No. Z20030007, number of production: 04080081, the content of DRTF ≥ 80%). Alpha-Minimum Essential Medium (α-MEM) was purchased from Life Technologies (USA). Fetal bovine serum (FBS) was obtained from ExCell Biology, Inc. (China). Ascorbic acid (AA), β–glycerophosphate (β-GP) and Alizarin Red S were purchased from Sigma-Aldrich (USA). Rat turnover markers ELISA kits were purchased from Biocalvin (Suzhou, China). RIPA lysis solution and a BCA protein assay kit were purchased from HEART biological technology Co., Ltd. (China). The RNAprep Pure Tissue Kit was purchased from TianGen Biotech Co., Ltd. (China). The PrimeScript™ RT reagent kit (Perfect Real Time) and SYBR Premix Ex Taq™ reagent were purchased from TAKARA Biotechnology (China). Anti-OPG antibody was purchased abcam (USA). Anti-ERα and anti-ERβ antibodies were purchased from R&D Systems (USA). Anti-GAPDH (Glyceraldehyde-3-phosphate dehydrogenase) antibody was obtained from Proteintech (China). Anti-RANKL and Horseradish peroxidase (HRP) conjugated antibodies were purchased from Ruiying bio (China).

2.2. Analysis the major constituents of DRTF

The naringin and neoeriocitrion in DRTF were identified by high performance liquid chromatography (HPLC), (LC-2010C, Shimadzu, Japan) and mass spectrometry (MS), (Esquire 6000, Bruker, Germany). The HPLC method was as follows: the reference solution was prepared by dissolving 1.69 mg naringin and 1.58 mg neoeriocitrin in 5 ml of methanol in a volumetric flask, separately. The DRTF samples were also dissolved in methanol and prepared as with the test solution. A 10 μl solution was subjected to HPLC and analyzed with a UV detector (SPD-M20A, Shimadzu, Japan) at 283 nm. The separating conditions were as follows: chromatographic column, MERCK C18 (4.6 × 250 mm, ID, 5 μm); column temperature, 30 °C; mobile phase was methanol (A): 0.2% acetic acid water (B). The gradient elution was as follows: 0–14 min, 30%–35% A; 14–22 min, 35%–50% A; 22–26 min, 50%–35% A; 26–35 min, and 35%–35% A, with a flow rate of 1.0 ml/min. The relative percentages of naringin and neoeriocitrin in the DRTF were calculated from area normalization of total chromatograms by a computerized integrator. The naringin and neoeriocitrin structures are shown in Fig. 1A and B. The MS identification conditions are as follows: the ion source was ESI, the atomization pressure was 35 psi, the dry gas flow rate was 11 ml/min, the drying temperature was 350 °C, the mass range of mass spectrometry were 100–1000 amu, and the ion mode was negative.

2.3. Animals and treatments

Three-month-old *Sprague–Dawley* specific pathogen-free female rats (SIPPR-BK Experimental Animal Ltd., body weight, 250 ± 20 g) were supplied by the Animal Center of the Fourth Military Medical University (Xi'an, China). The rats were housed with a 12/12 h light/dark cycle at 22 °C. During the experimental period, the rats were maintained on standard rodent chow and filtered water, which was available ad libitum. The acclimatized rats underwent either bilateral laparotomy (Sham, $n = 8$) or bilateral ovariectomy (OVX, $n = 40$). One week after recovering from surgery, the ovariectomized rats were randomly divided into five groups: OVX with vehicle (OVX, $n = 8$); OVX with E_2 (E_2, $n = 8$, 25 μg/kg body weight/day) or OVX with graded doses of DRTF (DRTF25, $n = 8$, 25 mg/kg body weight/day; DRTF75, $n = 8$, 75 mg/kg body weight/day and DRTF225, $n = 8$, 225 mg/kg body weight/day). Vehicle, E_2 and DRTF were all administered orally through a custom-made stomach tube, which lasted for 12 weeks. The body weights of the rats were recorded every two weeks to assess changes. The bone mineral content (BMC) and bone mineral density (BMD) were measured by dual-energy X-ray absorptiometry (DEXA) two days before the animals were euthanized. Urine samples were collected from the rats that were housed individually for 24 h in metabolic cages without providing food 1 day before euthanasia. Then, the samples were acidified with 2 ml 1 mol/l HCl. After the rats were anesthetized with pentobarbital sodium, a laparotomy was performed and blood samples were collected by abdominal aorta puncture from each anesthetized rat. Serum was then prepared by centrifugation (3000*g* for 10 min at 4 °C). Urine and serum samples were stored in aliquots at −80 °C for biochemical determinations. The uterus, heart, liver, spleen, lung, kidney, brain, and thymus were removed and weighed immediately. The uteri were put into 10% formalin solution for preservation. After 72 h of fixation, the uteri were paraffin embedded, sectioned and dyed with hematoxylin/eosin (HE). Femurs were dissected and placed in physiological saline and stored at −80 °C for bone biomechanical quality measurement with a three-point bending test. Additionally, trabecular bone microarchitecture was evaluated by micro-computed tomography (micro CT). All animals were treated in compliance with the principles and procedures contained in the most recent publication of the National Institutes of Health guide for the care and use of laboratory animals (NIH, 2011).

2.4. Assay for serum and urine chemistry

Serum calcium (S-Ca), serum phosphorus (S-P) and alkaline phosphatase (ALP) concentrations were measured by standard colorimetric methods using commercial kits (Nanjing Jiancheng Bioengineering Ltd., China) and analyzed with a multi-functional microplate spectrophotometer (SpectraMax M4, Molecular Devices, USA) (Zhai et al., 2014). Urine calcium (U-Ca), Urine phosphorus (U-P) and creatinine (Cr) concentrations were analyzed by the same method used for the serum samples. Urinary deoxypyridinoline (DPD), serum C-terminal telopeptide of type I collagen (CTX-I), osteocalcin (OC), propeptide of type I procollagen (PICP) and tartrate-resistant acid phosphatase (TRAP) levels were determined using rat ELISA kits (Biocalvin, Suzhou, China). Urinary Ca, P and DPD excretion were all expressed as the ratio to Cr concentration (Ca/Cr, P/Cr, DPD/Cr).

2.5. DEXA analysis

The BMD and BMC from whole animals were measured with a dual-energy X-ray absorptiometer (Lunar Prodigy Advance DEXA, GE healthcare, Madison, WI, USA) using the small laboratory animal scan mode (Pastoureau et al., 1995). The BMD and BMC values from the

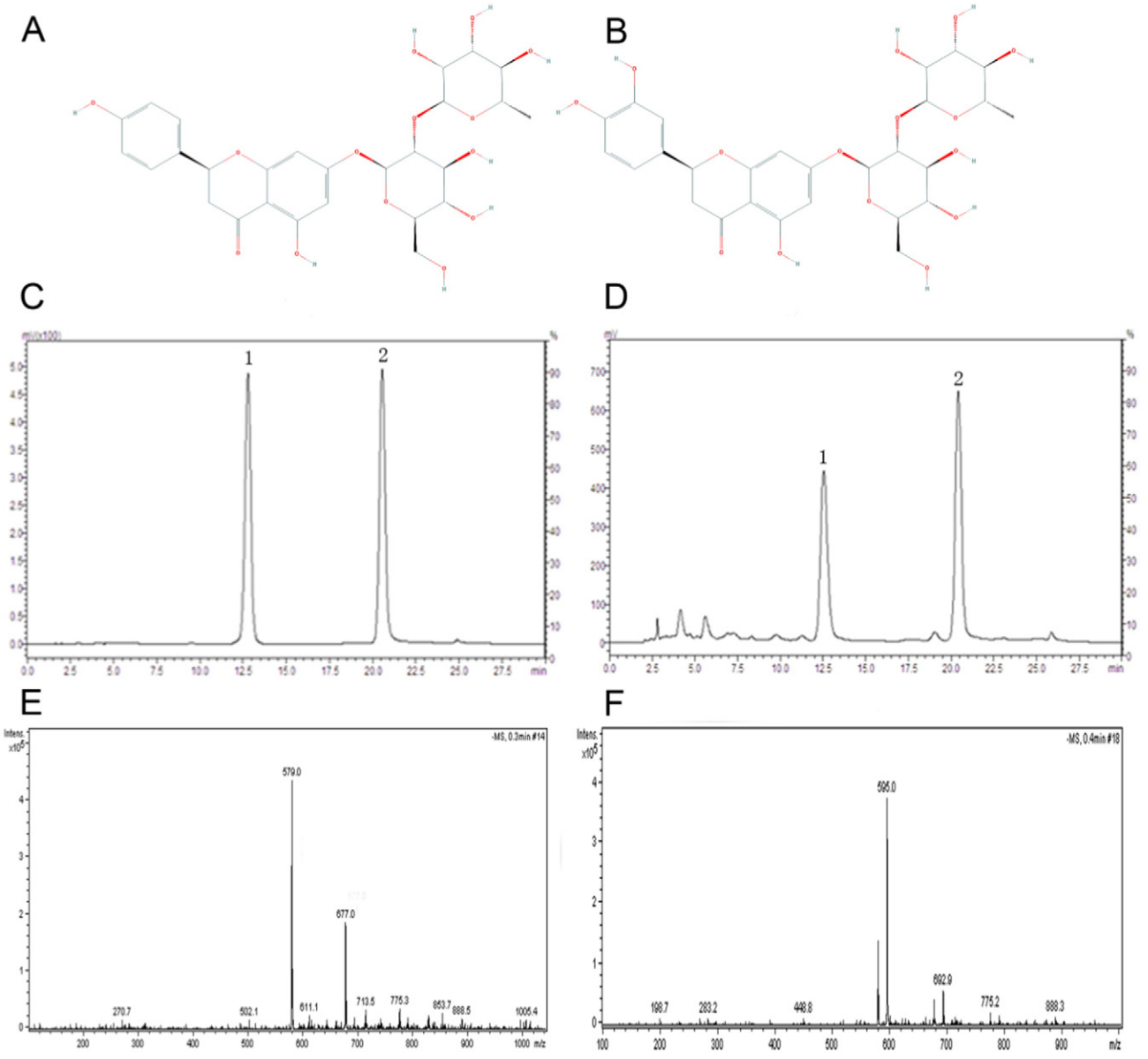

Fig. 1. The structures of naringin (A) and neoeriocitrin (B); the HPLC chromatograms of the reference substances (C) and DRTF (D). Peak 1 is neoeriocitrin, peak 2 is naringin; the primary mass spectrograms of naringin (E) and neoeriocitrin (F).

right femur were automatically calculated with purpose-designed software (enCORE™ 2006, GE Healthcare, Madison, WI, USA).

2.6. Three-point bending test

Prior to mechanical testing, the left femurs were removed from the freezer, submerged in physiological saline solution to thaw slowly, and held at room temperature on the day of testing. Then, each specimen was placed in a material testing machine on two supports that were separated by a distance of 20 mm and load was applied to the middle of the diaphysis, thus creating a three-point bending test. The biomechanical quality of the left femoral diaphysis was determined using AGS-10KNG material testing machine (SHIMADU, Japan) at a speed of 2 mm/min until fracture occurred. The central loading point was displaced, and the load and displacement values were recorded until the specimen was broken. From the load-deformation curve, the maximum load (ultimate strength, F_{max}), energy absorption (area under the curve, W_{abs}) and stiffness (slope of the linear region of the curve representing elastic deformation), maximum stress (F_{max}/cross-sectional area, σ_{max}) and Young's modulus values (maximum slope of the stress-strain curve, E) were obtained.

2.7. Micro CT analysis

The distal metaphysis in the right femur of each rat was scanned with Inveon micro CT (Siemens, Germany). The graphic image resolution was 1024 × 1024. Three-dimensional (3D) image data were acquired with a voxel size of 20 × 20 μm in all spatial directions with a micro CT evaluation program (V5.0A) (Laib et al., 2000). The volumes of interest (VOI), which were located 1 mm from the metaphyseal line to 2 mm (the 100 continuous slices) below it, were chosen for data analysis. The 3D segmented images were directly used to quantify microarchitecture with the Micro-View program (Siemens, Germany) and a multiple Intel® processors-based micro CT workstation. Morphological measurements were performed and the following 3D parameters were obtained by analyzing the VOIs for the trabecular bone: (1) the bone volume/tissue volume (BV/TV), (2) trabecular number (Tb.N), (3) trabecular thickness (Tb.Th), (4) trabecular separation

Table 1
The primer sequences of real time RT-PCR.

Gene	GeneBank no.	Primer sequences	Annealing temperature (°C)	Product length (bp)
OPG	NM_008764.3	Forward: 5′-CCAAAGTGAATGCCGAGAGT-3′	57	154
		Reverse: 5′-ACGCTGCTTTCACAGAGGTC-3′	57	
Rankl	NM_011613.3	Forward: 5′-CTCACCATCAATGCTGCCAG-3′	58	162
		Reverse: 5′-GCAAATGTTGGCGTACAGGT-3′	58	
ERα	NM_001302533.1	Forward: 5′-TGAAAGGCGGCATACGGAAA-3′	60	105
		Reverse: 5′-TGTCTCCTGAAGCACCCATT-3′	60	
ERβ	NM_010157.3	Forward: 5′-TAGAGAGCCGTCACGAATAC-3′	58	161
		Reverse: 5′-GGCTAAAGGAGAGAGGTGTC-3′	58	
GAPDH	NM_008084.2	Forward: 5′-AGGGCATCTTGGGCTACACT-3′	58	161
		Reverse: 5′-CACCCTGTTGCTGTAGCCGT-3′	58	

(Tb.Sp), (5) the trabecular pattern factor (Tb.Pf) and (6) cortical thickness (Cb.Th) (Marinozzi et al., 2013).

2.8. Cell culture

MC3T3-E1 cells were cultured in α-MEM medium supplemented with 10% FBS, 2.2 g/l sodium bicarbonate, 100 mg/ml streptomycin and100 Units/ml penicillin, in a humidified 37 °C, 5% CO_2 incubator. For cell differentiation experiments, confluent cells were cultured with osteogenic medium that contained α-MEM supplemented with 10% FBS, 100 mg/ml streptomycin, 100 units/ml penicillin, 50 mg/ml ascorbic acid and10 mM β-glycerophosphate (β-GP) and the medium was changed every 2 or 3 days.

2.9. Cell proliferation assay

Cell proliferation was determined with an MTT assay. MC3T3-E1 cells were seeded at a density of 2×10^3 cells/well in 96-well plates full of medium containing DRTF of various concentrations (0.1, 0.5, 2.5, 12.5, 62.5, or 312.5 μg/ml). After 24 and 48 h treatments, 20 μl of MTT solution (0.5 mg/ml) was then added into each well and the mixture was incubated for 4 h at 37 °C. Culture medium was then replaced with an equal volume of DMSO to dissolve the formazan crystals. After shaking at room temperature for 10 min, absorbance was measured at 570 nm with an Infinite M200 multifunctional microplate reader (Tecan, Austria). All experiments were performed in duplicate and repeated independently thrice.

2.10. Alkaline phosphatase activity

MC3T3-E1 cells were seeded at a density of 2×10^4 cells/well in 24-well plates with osteogenic medium in the presence or absence of DRTF (0.1, 0.5, 2.5, 12.5, 62.5, or 312.5 μg/ml). After 3 days, 6 days, 9 days and 12 days of treatment, cells were gently washed twice with PBS. Then, the cells were lysed with 0.2% Triton X-100 and the lysate was centrifuged at 15,000g for 5 min. The supernatant was collected for alkaline phosphatase (ALP) activity and protein concentration measurements with an ALP activity assay kit and a BCA-protein assay kit, respectively (Ehrlich et al., 2005; Yang et al., 2005).

2.11. Mineralized nodule measurement

Mineralization in MC3T3-E1 cells was determined by staining with Alizarin Red-S. Alizarin Red-S binds selectively to calcium and stains it dark red. Cells (2.5×10^4 cells/well) were seeded in 24-well plates and cultured with osteogenic medium with or without DRTF (12.5 μg/ml) during this period. The medium was changed every 2 days. After incubation for 12 days, the cells were washed with phosphate buffered saline (PBS, pH 7.4), fixed with 10% buffered formaldehyde for 15 min, rinsed with PBS and stained with 0.5% Alizarin Red S (pH 4.2) for 15 min at room temperature. After staining, the cells were washed with distilled water on a shaking platform for 5 min, 5 times. Images of the mineralized nodules were photographed using a microscope (TS100, Nikon, Japan). Image J software (National Institutes of Health, NIH) was used to quantify the area of mineralized nodules.

2.12. Real time RT-PCR analysis

MC3T3-E1 cells were seeded in 6-well plates at a density of 2×10^5 cells/well. After 2 days of culture, cells were treated with DRTF (2.5, 12.5, 62.5 μg/ml) for 12 h (6 wells per group). Total RNA was extracted from the treated cells using the RNAprep pure Tissue Kit according to the manufacturer's instruction. After the cells were washed twice with PBS, the concentration and purity of the RNA were determined by measuring the absorbance at 260 nm and 280 nm. The RNA samples (1000 ng) was reverse transcribed into complementary DNA (cDNA) using the PrimeScript™ RT reagent kit. The PCR amplification was carried out on LightCycler96 Thermal Cycler (Roche, USA) with specific primers and SYBR Premix Ex Taq™. The cycling parameters were as follows: pre-denaturation at 95 °C for 30 s, followed by 45 cycles of 95 °C for 10 s, 57 °C, 58 °C or 60 °C for 15 s, and 72 °C for 10 s. Following the PCR reaction, melting curve analysis was conducted to verify the specificity and identity of the PCR product. Ct values for the samples were normalized to that of GAPDH and the relative expression was calculated via the $2-\Delta\Delta Ct$ method (Chang et al., 2009; Lau et al., 2008). All reactions were carried out in triplicate. The primer sequences are given in Table 1.

2.13. Western blotting

MC3T3-E1 cells were treated with DRTF (12.5 μg/ml). After 24 h of incubation, cells were washed with PBS and lysed in RIPA lysis solution. The cell lysates were centrifuged at 10,000 RPM for 10 min at 4 °C. The supernatants were collected and the total protein content was quantified with a BCA assay kit. Then, 15 μg of total protein from each sample was separated by SDS-PAGE (10% gel) and transferred to PVDF membranes. After incubation in blocking solution (5% non-fat milk, 0.05% Tween-20 in TBS) for 2 h at room temperature, the membrane was incubated with an appropriate primary antibody against OPG, RANKL, ERα, ERβ and GAPDH at 4 °C overnight. After three washes with TBS containing 0.05% Tween-20 (TBST), the membranes were incubated with horseradish peroxidase (HRP) conjugated secondary antibody for 2 h at room temperature. Next, the immunoreaction signals were detected with the enhanced ECL chemiluminescence reagent kit (Biodragon-immunotech, China) and exposed on Gel Doc™ XR + System (Bio-Rad, USA). The relative protein intensities were quantified using Quantity One 1-D analysis software (Bio-Rad, USA) and GAPDH was used as internal control.

2.14. Statistical analysis

Data are presented as the mean ± standard deviation (SD). One-way ANOVAs were used to compare data from all groups and Turkey's tests were used as a post-test to compare pairs of groups with the SPSS 16.0 statistical software (SPSS Inc., Chicago, IL, USA). Differences

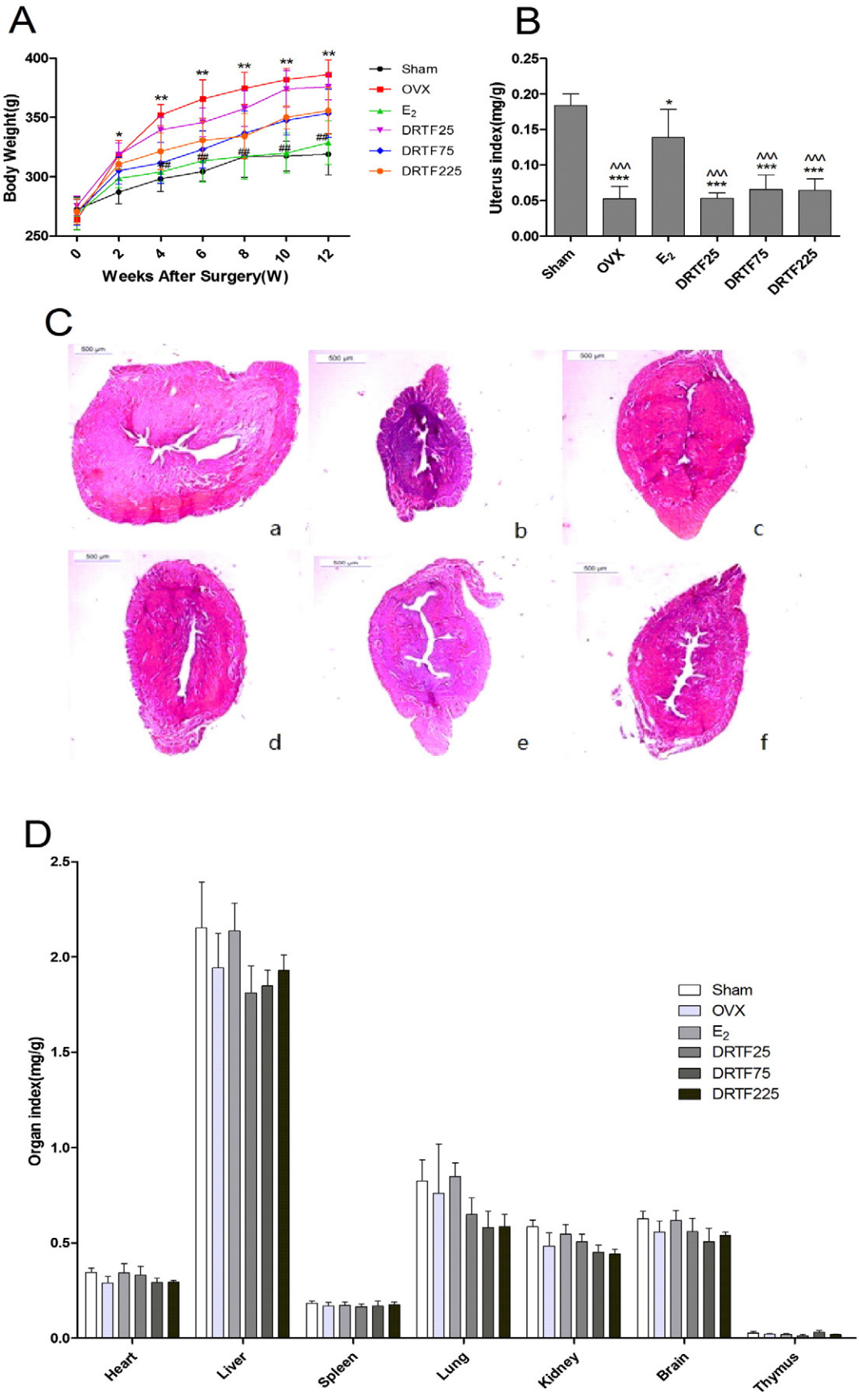
A
Body Weight(g)
Weeks After Surgery(W)
Sham
OVX
E2
DRTF25
DRTF75
DRTF225
B
Uterus index(mg/g)
C
a
b
c
d
e
f
D
Organ index(mg/g)
Heart
Liver
Spleen
Lung
Kidney
Brain
Thymus

Table 2
Effects of TL on biochemical parameters in serum and urine of rats.

Parameters	Sham	OVX	E_2	TFDF25	TFDF75	TFDF225
S-Ca (mmol/l)	1.77 ± 0.18	1.79 ± 0.12	1.91 ± 0.31	1.74 ± 0.12	1.71 ± 0.03	1.69 ± 0.09
S-P (mmol/l)	1.48 ± 0.27	1.74 ± 0.51	1.85 ± 0.26	1.68 ± 0.25	1.47 ± 0.12	1.64 ± 0.20
U-Ca/Cr (mmom/mmol)	0.22 ± 0.05	0.39 ± 0.03**	0.24 ± 0.05##	0.29 ± 0.04#	0.29 ± 0.38#	0.27 ± 0.04##
U-P/Cr (mmom/mmol)	2.63 ± 0.50	3.83 ± 0.40**	3.01 ± 0.43##	3.17 ± 0.44	3.07 ± 0.43#	2.97 ± 0.45##
U-DPD/Cr (nmom/mmol)	50.23 ± 8.05	80.42 ± 6.45**	55.18 ± 3.72##	68.18 ± 5.39**	62.23 ± 3.90*,#	60.08 ± 6.95*,#
Trap (U/l)	3.07 ± 0.45	5.31 ± 0.75**	3.41 ± 0.74##	4.00 ± 0.62#	3.98 ± 0.42#	3.63 ± 0.81##
CTX-I (ng/ml)	2.89 ± 0.25	4.89 ± 0.43**	3.35 ± 0.39##	4.17 ± 0.51	3.63 ± 0.49##	3.28 ± 0.59##
OC (ng/ml)	2.24 ± 0.08	3.26 ± 0.29**	2.41 ± 0.41##	2.74 ± 0.25#	2.62 ± 0.15##	2.55 ± 0.24##
ALP (U/100 ml)	1.20 ± 0.38	2.34 ± 0.72**	1.36 ± 0.311##	1.74 ± 0.3	1.38 ± 0.37#	1.31 ± 0.22##
PICP (ng/ml)	2.49 ± 0.22	4.33 ± 0.56**	2.47 ± 0.41**	3.11 ± 0.49*	2.93 ± 0.45**	2.63 ± 0.36**

Note. Values are mean ± SD ($n = 8$).
* $p < 0.05$ vs. Sham.
** $p < 0.01$ vs. Sham.
\# $p < 0.05$ vs. OVX.
\#\# $p < 0.01$ vs. OVX.

between means were considered statistically significant when p-values < 0.05.

3. Results

3.1. Quality assessment of DRTF extract

Naringin (Fig. 1A) and neoeriocitrion (Fig. 1B), which are two flavonoids, were the main ingredients observed in the Drynariae Rhizoma. Naringin is a commonly used marker for authentication of Drynariae Rhizoma extract, according to the Chinese pharmacopoeia (China, 2015). In our research, naringin and neoeriocitrion were identified by standard substance and mass spectrometry analysis. Fig. 1C is the typical chromatography profile of the two standards in which neoeriocitrion showed a high peak at retention time 12.54 min and naringin showed a high peak at retention time 20.41 min. A typical HPLC chromatogram profile of the DRTF is shown in Fig. 1D. The chemical formula of naringin is $C_{27}H_{32}O_{14}$ and its molecular weight is 580.54. The chemical formula of neoeriocitrion is $C_{27}H_32O_{15}$ and its molecular weight is 596.174. Therefore, the ESI-MS m/z for naringin is 579 $[M\text{-}H]^-$ and the ESI-MS m/z for neoeriocitrion is 595 $[M\text{-}H]^-$. The primary mass spectrograms of naringin and neoeriocitrion are shown in Fig. 1E and F. Based on the normalization areas of the total chromatograms, the relative percentage of naringin and neoeriocitrin in the DRTF were 32.92% and 43.43%, respectively.

3.2. Body and organ weights

The rats from six experimental groups had similar initial mean body weights ($p > 0.05$). The body weights of all groups were increased under the pair feeding conditions. The results showed that the growth rate of the OVX group was higher than that of the Sham group ($p < 0.01$) on week 4 after surgery, which also lasted throughout the experiment. E_2 prevented increased body weight and returned the body weight near to the level maintained by Sham group 4 weeks after treatment ($p < 0.01$). DRTF (25 mg/kg/day) did not influence body weight, while DRTF (75 and 225 mg/kg/day) decreased the body weight to some degree 4 weeks later (Fig. 2A). Additionally, OVX caused significant atrophy of uterus compared with the Sham group ($p < 0.001$), indicating the success of the surgical procedure. Administering E_2 significantly increased the uterine weight compared with the OVX group ($p < 0.001$). On the contrary, none of the DRTF doses elicited the uterotropic effects of E_2 (Fig. 2B and C). The heart, liver, spleen, lung, kidney, brain and thymus organ indices were not significantly different among the groups (Fig. 2D).

3.3. Biochemical assay

The biochemical serum and urine parameters from all groups are shown in Table 2 (Delmas et al., 2000). The OVX treatment did not alter the S–Ca and S–P levels between all groups ($p > 0.05$ for all). Nevertheless, the U–Ca and U–P levels in the OVX group were significantly increased compared with the Sham group ($p < 0.01$). Treatment with either DRTF or E_2 significantly prevented the OVX-induced increase in U-Ca/Cr and U-P/Cr levels ($p < 0.05$ or $p < 0.01$). Twelve weeks after OVX treatment, bone resorption markers such as urinary DPD/Cr ratio, plasma TRAP (Bonjour et al., 2012; de la Piedra et al., 1997), CTX-I, and bone formation markers for plasma OC, ALP and PICP (Miura et al., 1995) were measured, and all the tested parameters were significantly increased in OVX group ($p < 0.01$), However, the DRTF and E_2 treatments prevented the OVX-induced increase in the biochemical markers mentioned above ($p < 0.05$ or $p < 0.01$). These results indicated that DRTF or E_2 could prevent the OVX-induced increase in the bone turnover rate in rats.

3.4. BMD and BMC evaluation

There were no differences in the right femur BMC values between all of the treatment groups. However, The BMD was significantly lower in the OVX group compared with the Sham group ($p < 0.001$). The twelve-week DRTF treatment at higher doses (75 or 225 mg/kg/day) and the E_2 treatment significantly increased the right femur BMD levels compared with the OVX group ($p < 0.01$) (Fig. 3).

3.5. Biomechanical quality test

A three-point bending test was performed to determine the effects of DRTF on rat femur bone strength (Ederveen et al., 2001). As shown in Table 3, after 12 weeks of estrogen deficiency, the max-load values in OVX group reduced significantly. The levels of energy and stiffness in OVX group tended to decrease, however, they did not reach statistical significance compared with the Sham group. Although the E2 and DRTF treatments altered the max-load, energy and stiffness levels, neither E_2 nor DRTF had significant effects on the values of these three biomechanical parameters compared with OVX group. However, the OVX treatment significantly reduced the max-stress and Young's

Fig. 2. Effects of DRTF or E_2 on body weights and organ indices in OVX rats. (A) The body weights of the animals were recorded every 2 weeks during the experimental period. Values are mean ± SD ($n = 8$), *$p < 0.05$, **$p < 0.01$compared with sham; \#$p < 0.05$, \#\#$p < 0.01$ compared with OVX. (B) Uteri were isolated and weighed after euthanization, the uterus index was determined as the uterus weight divided by body weight. Values are mean ± SD (n = 8), *$p < 0.001$, ***$p < 0.001$ compared with sham; ^^^$p < 0.001$ compared with E_2 treatment. (C) HE dyed sections of rat uteri obtained from (a) Sham, (b) OVX, (c) E_2, (d) DRTF25, (e) DRTF75, and (f) DRTF225 treated animals. (D) The heart, liver, spleen, lung, kidney, brain and thymus were isolated and weighed after the animals were sacrificed and the organ index was represented as organ weight divided by body weight.

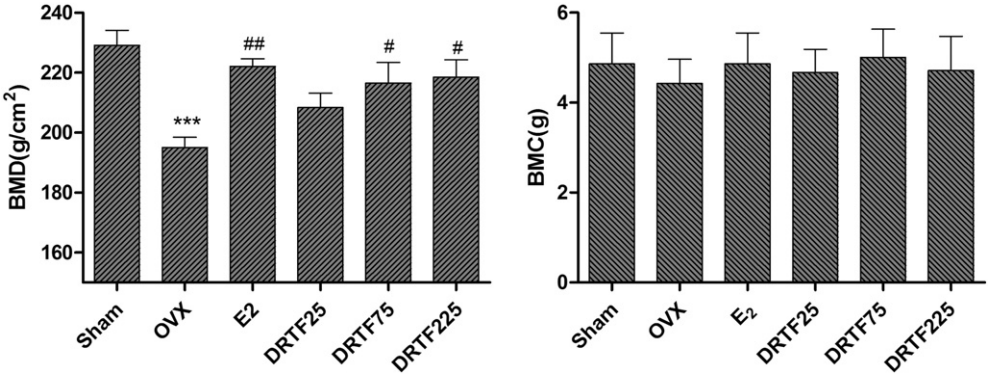

Fig. 3. Effects of 12-week treatment on the BMD and BMC in the femur of OVX rats by DEXA. Values are mean ± SD ($n = 8$), $^{***}p < 0.001$ different from Sham; $^{\#}p < 0.05$, $^{\#\#}p < 0.01$ different from OVX.

Table 3
Effects of 12-week DRTF treatment on biomechanical parameters in the femoral diaphysis of rats.

Parameters	Sham	OVX	E_2	TFDF25	TFDF75	TFDF225
Max-load [N]	129.68 ± 13.52	111.23 ± 3.53*	124.19 ± 12.97	115.73 ± 5.99	118.60 ± 6.09	121.64 ± 8.59
Energy [N·mm]	102.09 ± 10.09	87.63 ± 5.35	97.40 ± 4.92	86.29 ± 6.19	88.12 ± 13.20	91.84 ± 6.52
Stiffness [N/mm]	209.08 ± 19.41	188.58 ± 10.95	204.02 ± 14.37	183.42 ± 17.31	198.32 ± 13.52	203.88 ± 12.94
Max-stress [MPa]	84.39 ± 6.49	67.01 ± 4.35**	81.05 ± 11.68#	71.21 ± 4.16	78.98 ± 5.80#	80.12 ± 4.76#
Young's modulus [MPa]	2244.41 ± 255.09	1703.88 ± 178.05**	2193.72 ± 222.64##	1976.55 ± 153.34	2088.63 ± 175.61#	2146.02 ± 291.95#

Note. Values are mean ± SD ($n = 8$).
* $p < 0.05$, different from Sham.
** $p < 0.01$, different from Sham.
\# $p < 0.05$, different from OVX.
\#\# $p < 0.01$, different from OVX.

modulus ($p < 0.01$). Compared with the OVX group, treatment with E_2 or DRTF (75 or 225 mg/kg/day) significantly prevented the decreases in max-stress and Young's modulus in the OVX rats ($p < 0.05$ or $p < 0.01$).

3.6. Micro CT evaluation

Three-dimensional images of femoral metaphysis showed differences in trabecular microarchitecture amongst the various treatment groups, as represented in Fig. 4A–F. Analysis of the representative samples indicated that OVX significantly decreased the trabecular BV/TV, Tb.N, and Tb.Th levels ($p < 0.001$) compared with the Sham group. In contrast, the distal femur Tb.Sp and Tb.Pf levels in the OVX rats were significantly increased compared with the Sham group ($p < 0.01$). Compared with the OVX group, the DRTF (75 or 225 mg/kg/day) or E_2 treatments reversed the effects mentioned above at some degree amongst all of the groups. Nevertheless, the thickness of cortical bone had no significant difference in each group (Table 4).

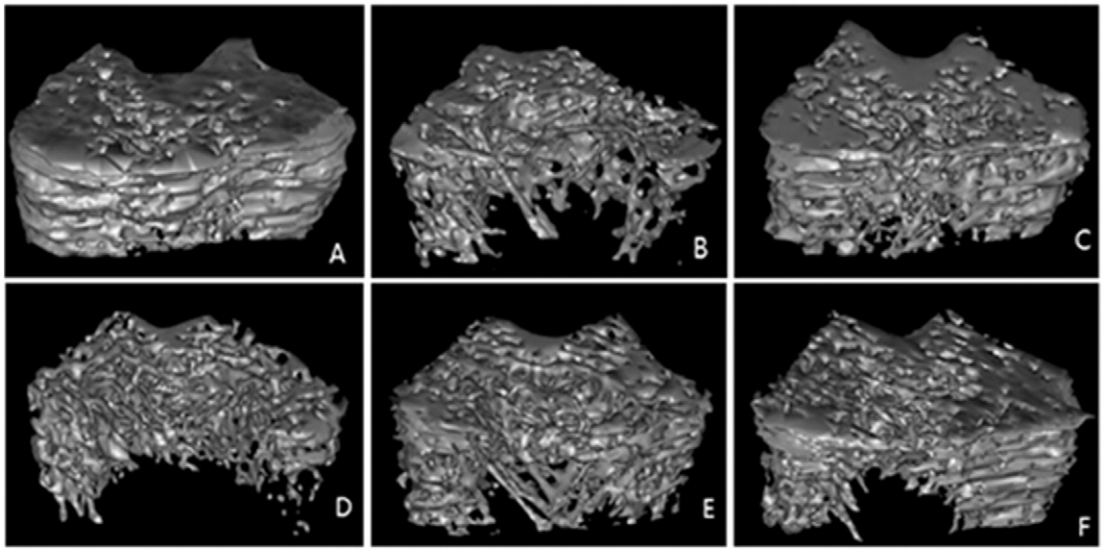

Fig. 4. Representative sample from each group: 3D architecture of trabecular bone within the distal metaphyseal femur region: (A) Sham, (B) OVX, (C) E_2, (D) DRTF25, (E) DRTF75, (F) DRTF225.

Table 4
Micro CT 3D parameters of trabecular bone in the distal femur region.

Parameters	Sham	OVX	E_2	DRTF25	DRTF75	DRTF225
BV/TV (%)	0.54 ± 0.04	0.31 ± 0.06***	0.45 ± 0.04##	0.35 ± 0.04**	0.42 ± 0.04#	0.42 ± 0.02#
Tb.Th (mm)	0.12 ± 0.02	0.08 ± 0.01***	0.12 ± 0.01##	0.10 ± 0.01	0.11 ± 0.01#	0.11 ± 0.01#
Tb.N (1/mm)	5.12 ± 0.14	2.89 ± 0.11***	4.66 ± 0.50###	3.79 ± 0.13	4.33 ± 0.29**	4.49 ± 0.46##
Tb.Sp (mm)	0.02 ± 0.01	0.19 ± 0.05**	0.10 ± 0.02#	0.16 ± 0.02	0.11 ± 0.04#	0.10 ± 0.02#
Tb.Pf (1/mm)	4.66 ± 0.65	8.32 ± 1.00**	5.06 ± 0.84#	6.67 ± 0.75	5.41 ± 0.80#	5.04 ± 0.39#
Ct.Th (mm)	0.48 ± 0.002	0.45 ± 0.02	0.46 ± 0.02	0.45 ± 0.02	0.46 ± 0.01	0.46 ± 0.03

Note. Values are mean ± SD ($n = 8$).
** $p < 0.01$, different from Sham.
*** $p < 0.001$, different from Sham.
# $p < 0.05$, different from OVX.
$p < 0.01$, different from OVX.
$p < 0.001$, different from OVX.

3.7. Effects of DRTF on the differentiation of MC3T3-E1 cells

The cell proliferation rates, as measured by the MTT assay, were significantly increased when the cells were treated with DRTF (12.5 or 62.5 μg/ml) ($p < 0.01$ for all) (Fig. 5). Based on this preliminary observation, we evaluated the differentiation-inducing activities of DRTF on MC3T3-E1 cells by assessing ALP activity. ALP activity is a phenotypic marker for early differentiation of osteoblasts. When MC3T3-E1 cells were treated with different concentrations (0.1, 0.5, 2.5, 12.5, 62.5, 312.5 μg/ml) of DRTF for different time points, the ALP activity increased in a time-dependent manner, with a maximum activity level observed on the 9th day; however, it decreased on the 12th day. DRTF (12.5 or 62.5 μg/ml) exhibited significant stimulating effects on cell differentiation ($p < 0.01$ or $p < 0.05$), while it decreased cell differentiation at 312.5 μg/ml. As the strongest activity obtained by the above experiments was 12.5 or 62.5 μg/ml, this concentration was used in the following experiments.

3.8. Effects of DRTF on MC3T3-E1 cell maturation

The formation of mineralized nodules is one of the important markers during osteoblastic maturation. MC3T3-E1 cells were incubated with DRTF (12.5 μg/ml) in osteogenic medium for 12 days and stained with Alizarin Red S to detect mineralized nodule formation, as represented by bright red color. The mineralized areas in MC3T3-E1 cells cultured with DRTF showed remarkably increased intensity compared with the control (Fig. 6). In addition to the obvious color change, the amount of mineralized nodules following DRTF treatment was significantly higher than that of the control ($p < 0.01$).

3.9. Effects of DRTF on OPG and RANKL expression

Osteoprotegrin (OPG) and receptor activator of NF–κB ligand (RANKL) were identified as the dominant and final mediators of

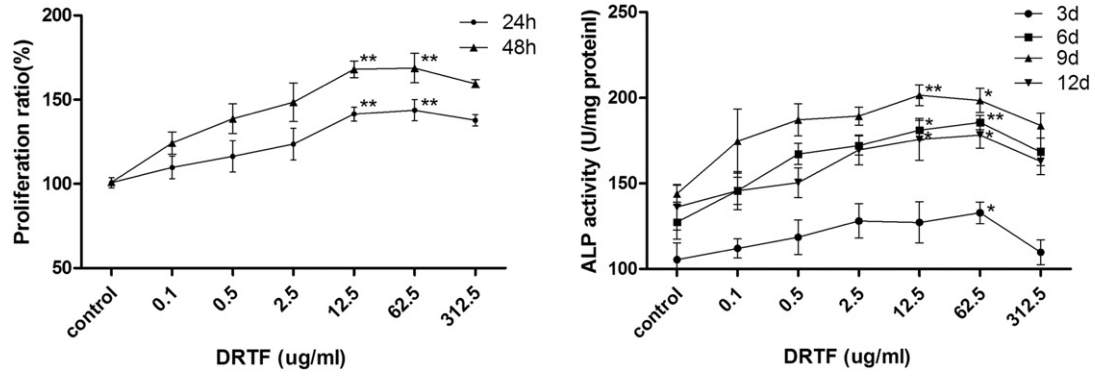

Fig. 5. Effects of DRTF on the proliferation and differentiation of MC3T3-E1 cells: (A) Cell proliferation of MC3T3-E1 was evaluated by the MTT method. Values are mean ± SD ($n = 8$), **$p < 0.01$ vs. control. (B) ALP activity was assessed using Alkaline Phosphate Assay Kit. Values are mean ± SD ($n = 8$), *$p < 0.05$, **$p < 0.01$ vs. control.

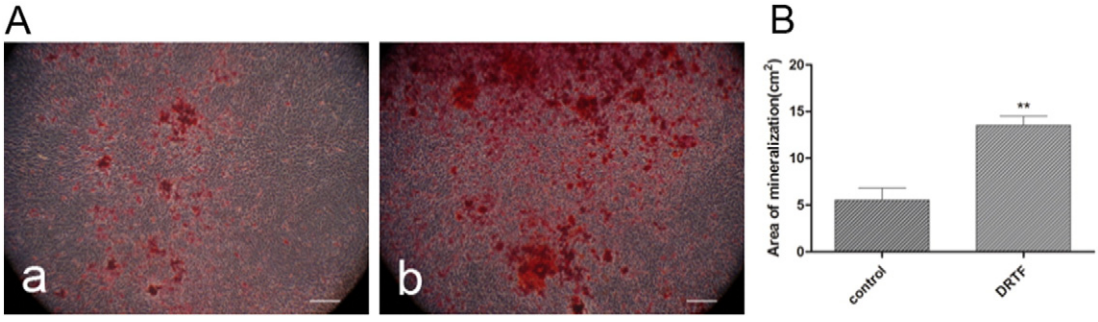

Fig. 6. Mineralized nodules formation of MC3T3-E1 cells cultured with osteogenic medium. (A) Representative images of mineralized nodules stained by Alizarin Red S, (a) DMEM control, (b) DRTF (12.5 μg/ml) treatment, bar: 100 μm. (B) Quantitative analysis of the area of mineralized nodules using Image J software. Values are mean ± SD ($n = 3$), **$p < 0.01$ vs. control.

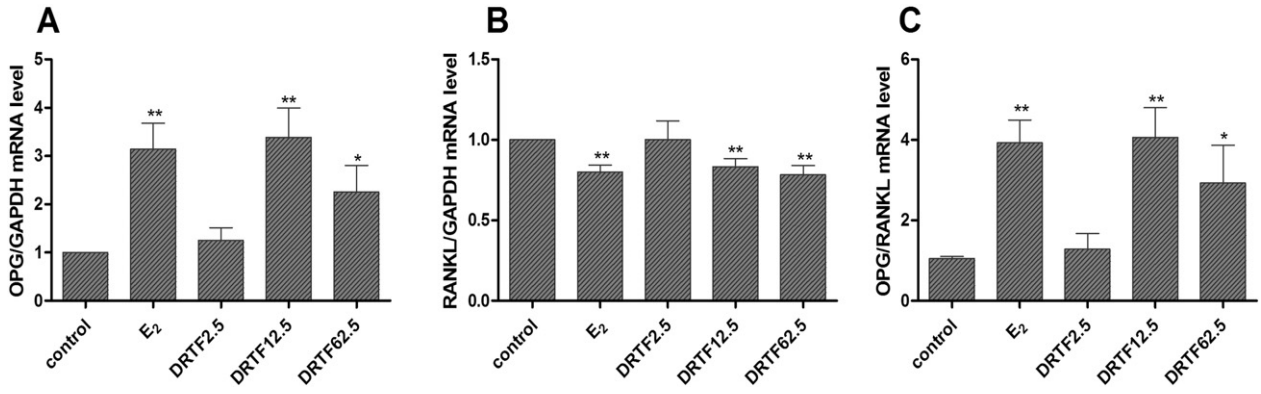

Fig. 7. Effects of DRTF on *OPG* and *RANKL* mRNA expression in MC3T3-E1 cells. MC3T3-E1 cells were treated with vehicle (control), E_2 and different concentrations of DRTF (2.5, 12.5 and 62.5 μg/ml) for 12 h. Total RNA was isolated and real-time RT-PCR was performed to determine the mRNA expression levels of *OPG* (A) and *RANKL* (B), which were normalized to that of *GAPDH*. The results are expressed as the mean ± SD ($n = 3$). (C) Effect of DRTF on the *OPG*/*RANKL* message level ratio in MC3T3-E1 cells. Data are presented as the mean ratio of *OPG*:*RANKL* expression ± SD ($n = 3$). $^{*}p < 0.05$, $^{**}p < 0.01$ vs. control.

osteoclastogenesis (Bord et al., 2003; Zhang et al., 2014b). As shown in Fig. 7A, DRTF at 12.5 and 62.5 μg/ml significantly increased *OPG* expression in MC3T3-E1 cells ($p < 0.01$ or $p < 0.05$). On the contrary, *RANKL* expression was down-regulated following DRTF treatment ($p < 0.01$) (Fig. 7B). The *OPG* to *RANKL* ratio was then calculated to demonstrate its effects on osteoclastogenesis. The results showed that the ratio was significantly increased in the DRTF group (12.5 and 62.5 μg/ml) compared with the control ($p < 0.01$ or $p < 0.05$) (Fig. 7C).

We then detected the protein production of OPG and RANKL in the presence and absence of DRTF (12.5 μg/ml) using western blotting (Fig. 8). The results were consistent with the gene expression levels, which indicated that DRTF can inhibit osteoclastogenesis by decreasing the direct interaction between RANKL expression on osteoblasts and RANK expression on the osteoclast cell surface.

3.10. Effects of DRTF on ERα and ERβ expression

To determine whether DRTF could alter ER expression, the *ERα* and *ERβ* expression levels were studied. Our results indicated that E_2 (10^{-11} M) activated ER-dependent transcription activity via *ERα* ($p < 0.01$ vs. control) as well as *ERβ* ($p < 0.001$ vs. control). Additionally, DRTF increased the *ERα* and *ERβ* expression levels in a concentration dependent manner. DRTF at concentration of 12.5 and 62.5 μg/ml significantly enhanced *ERα* and *ERβ* expression in the MC3T3-E1 cells (Fig. 9A, B, $p < 0.05$ or $p < 0.01$ vs. control).

Moreover, we examined the protein production of ERα and ERβ in the presence or absence of DRTF using western blotting. As shown in Fig. 10A, E_2 and DRTF (62.5 μg/ml) significantly up-regulated ERα and ERβ expression in the MC3T3-E1 cells (Fig. 10B, $p < 0.05$ or $p < 0.01$ vs. control).

4. Discussion

Drynariae Rhizoma and other kidney-tonifying traditional Chinese medicines have been widely used for thousands of years to treat fractures and joint diseases. In the present study, we evaluated the skeletal effects of DRTF on osteoporotic rats and explored the possible osteogenic effect mechanisms.

In order to evaluate the positive DRTF-mediated effects for the treatment of PMOP, the internationally accepted OVX rat model was utilized in this study (Nakamuta, 2004). As expected, OVX resulted in a significant reduction in the total BMD in the femur after 12 weeks. This loss in bone mass was accompanied by a significant simultaneous increase in bone remodeling, as was demonstrated by the enhanced bone turnover marker levels, such as Ca/Cr, P/Cr, DPD/Cr, CTX-I, PICP, OC, ALP and Trap. These results suggested that OVX alters calcium metabolism

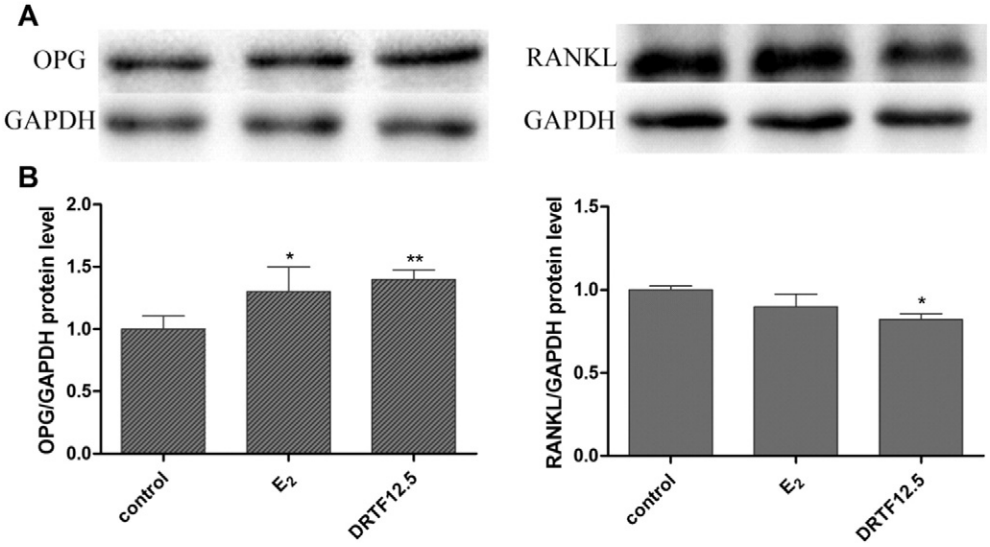

Fig. 8. Effects of DRTF on the OPG and RANKL protein levels in MC3T3-E1 cells. (A) Western blot analysis of OPG and RANKL expression after treatment of MC3T3-E1 cells with E_2 or DRTF (12.5 μm/ml) for 48 h. (B) "Quantity one" from Bio-Rad was used to analyze the western blot results, the values represent mean ± SD ($n = 3$), $^{*}p < 0.05$, $^{**}p < 0.01$ vs. control.

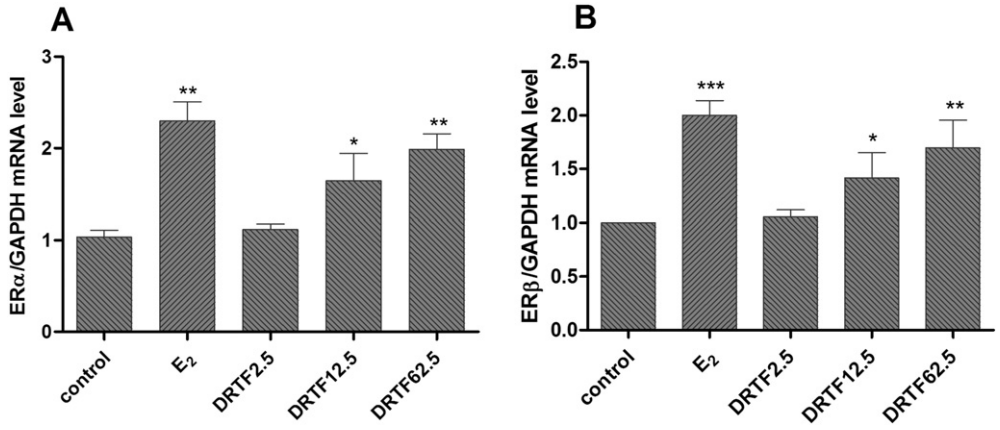

Fig. 9. Effects of DRTF on *ERα* and *ERβ* mRNA expression in MC3T3-E1 cells. MC3T3-E1 cells were treated with vehicle (control), E_2 and different concentrations of DRTF (2.5, 12.5 and 62.5 μg/ml) for 12 h. Total RNA was isolated and real-time RT-PCR was performed to determine the mRNA expressions levers of *ERα* (A) and *ERβ* (B), which were normalized to that of *GAPDH*. The results were expressed as the mean ± SD ($n = 3$), $^{*}p < 0.05$, $^{**}p < 0.01$ vs. control.

and causes a significant increase in bone turnover rate. Treatment with DRTF or E_2 prevented the decreased total BMD levels, which were reflected by the decreased bone turnover markers mentioned above. In summary, these results indicate a reduction in the bone turnover rate after treatment with DRTF and E_2.

Although such inhibition would generally be considered beneficial, biomechanical bone competence may be compromised if bone remodeling is excessively inhibited (Ederveen et al., 2001). Therefore, the three-point bending test was carried out to investigate the effects of DRTF on the biomechanical properties of the femurs from the OVX rats. Structural biomechanical properties (i.e., maximum load, stiffness and energy) are influenced by bone material properties and by the bone architecture or geometric properties, which are called extrinsic biomechanical properties. The actual effect from the treatment with regard to biomechanical competence can only be fully evaluated by material biomechanical parameters such as maximum stress and Young's modulus, which are called intrinsic biomechanical properties (Turner and Burr, 1993). From a biomechanical point of view, an ideal drug for bone fragility treatment should improve bone strength and decrease brittleness, in order to improve the extrinsic biomechanical properties of the bone but not substantially impair its intrinsic properties (Zhang et al., 2014a). In fact, it is very difficult to achieve this combination of effects. Fluoride treatment is a good example, as fluoride can improve bone mass (Haguenauer et al., 2000); however, fluoride incorporation into bone mineral reduces its intrinsic biomechanical properties (Turner et al., 1995). Our data confirmed that it is difficult to simultaneously improve the intrinsic and extrinsic properties. After 12 weeks of daily treatment, the DRTF or E_2 treatments only promoted the intrinsic properties of the femur. The improvement in the intrinsic properties may be due to the trabecular bone structure optimization.

Preservation of the trabecular bone architecture significantly promotes bone strength and may be more important in decreasing fracture risk than improving BMD (Bouxsein, 2003). Therefore, microarchitecture determinants are necessary to evaluate the true impact of a treatment on trabecular bone quality (Marinozzi et al., 2013; Muller et al., 2004; Wronski et al., 1989). The results of the micro CT indicated that the morphometric parameters (BV/TV, Tb.Th and Tb.N) of the trabecular bone at the distal femur were improved in the OVX rats in response to 12 weeks of daily oral treatment with DRTF. Furthermore, the DRTF treatment decreased the ovariectomy-induced alterations of the Tb.Sp and Tf.Pf, indicating that the deterioration of the microstructural geometry of the trabecular bone was largely prevented. Although we observed some positive effects from the DRTF treatments on the trabecular bone micro-architectural properties, none of the treatments,

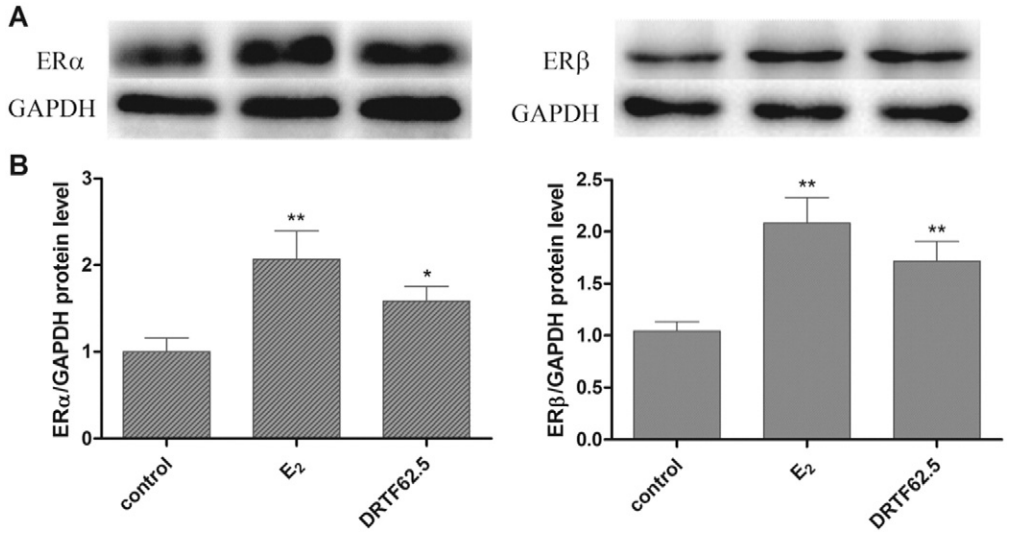

Fig. 10. Effects of DRTF on the ERα and ERβ protein level in MC3T3-E1 cells. (A) Western blot analysis of ERα and ERβ expressions after treatment of MC3T3-E1 cells with E_2 or DRTF (62.5 μm/ml) for 48 h. (B) "Quantity one" from Bio-Rad was used to analyze the western blotting results. The values were expressed as mean ± SD ($n = 3$), $^{*}p < 0.05$, $^{**}p < 0.01$ vs. control.

including E_2, were able to restore the deteriorated trabecular bone (Devareddy et al., 2006). These findings are consistent with those of other studies in which the trabecular structure restoration were unable to be observed after its deterioration had occurred, emphasizing the need for trabecular bone loss prevention (Laib et al., 2001).

The in vitro study using MC3T3-E1 cells provided further support for the potential action of DRTF on bone. DRTF not only promoted proliferation and increased ALP activity but it also enhanced the formation of mineralized nodules in osteoblasts. These results indicated that DRTF might participate in multiple stages of the osteoblast differentiation process, from early to terminal stages, to stimulate osteoblast cell differentiation and maturation. We also determined the expression of several important proteins that are involved in the osteoblast differentiation process as well as osteoclastogenesis in bone, such as OPG, RANKL, ERα and ERβ. With the recent discovery of RANKL–RANK interaction, the role of osteoblasts in osteoclast differentiation is now clearly defined. Binding of RANKL secreted from osteoblastic cells to RANK on the osteoclast cell surface results in an induction of osteoclast function, whereas, the secretion of OPG (the soluble decoy receptor of RANKL) by osteoblasts can interfere with RANKL–RANK interactions, which inhibits osteoclastogenesis (Boyce and Xing, 2008; Theoleyre et al., 2004). The present study showed that DRTF (12.5 μg/ml) stimulated OPG and suppressed RANKL expression, leading to an increased expression ratio of OPG/RANKL in ME3T3-E1 cells, which might inhibit osteoclastogenesis via modulation of the OPG/RANKL system in osteoblastic cells. Furthermore, previous studies reported that DRTF can up-regulate bone-related gene expression that are involved in bone formation (such as Smad1 and Smad5) (Zhu et al., 2010), suppress the circulatory level of cytokines involved in inducing bone resorption (TNF-α and IL-6), and stimulate cytokines (i.e., IL-4) associated with bone resorption suppression in OVX rats (Xie et al., 2004; Zhu et al., 2010).

Estrogen is one of the most important hormones in the body. It is primarily secreted by the ovaries, testicle and hypothalamus and plays a physiological role by binding two ER subtypes (ERα and ERβ). ERβ is more abundant in bone tissue while ERα is mainly distributed in reproductive cells, especially those of the breast and uterus. A previous study showed that the presence of ERβ-like immunoreactivity in the nuclei of human and murine osteoblasts and osteocytes and in the cytoplasm of osteoclasts and chondrocytes (Kuiper et al., 1998). Supplemental estrogen can inhibit osteoclast activity and reduce high bone turnover rate. Additionally, long-term supplement can increase estrogen levels, resulting in hyperplasia of the endometrium and ductal epithelial cells, which can increase the risk of breast and uterine cancer (Hvidtfeldt et al., 2015). Although the osteo-protective effects of DRTF in vivo were similar to those of E_2 as reported in studies by others (Magnusson and Weiderpass, 2001; Morch et al., 2012; Morch et al., 2009), DRTF did not mimic the effects of E_2 on uterus weight. Moreover, DRTF is also safe for the body, as the organ indexes were not significantly different amongst the groups. The in vitro study showed that DRTF (62.6 μg/ml) improved both ERα and ERβ expression levels in the MC3T3-E1 cells. The results demonstrated that DRTF behaves as a phytoestrogen and exerts positive effects in bone cells via ER-dependent pathways. The mechanism of the action of the phytoestrogens is similar to the estrogen, which then combines with the estrogen receptor, acts on the estrogen response element in the nucleus, and exerts its physiological function (Boonchird et al., 2010).

In conclusion, DRTF administration was able to prevent estrogen deficiency induced bone mass decrease and deterioration of trabecular microarchitecture without hyperplastic effects on the uterus and other organs, thus maintaining the structural integrity and biomechanical qualities of the bone. Moreover, DRTF appeared to exert positive effects on bone formation, while negatively modulating bone resorption. These effects seem to be related to the high content of flavonoids that behave as phytoestrogens but did not act the same as estrogen. Our study may provide evidence to support the use of DRTF as a reasonable alternative for the prevention and treatment of PMOP.

5. Conclusions

In this study, we systematically evaluated the protective effects of DRTF on OVX-induced bone loss in female rats and explored the possible mechanism of their therapeutic effects. The data demonstrated that DRTF could prevent OVX-induced bone loss without uterine estrogenic effects. Such a bone-protective role makes it a promising alternative agent for the safe and effective treatment of PMOP. As the major active ingredients in DRTF are naringin and neoeriocitrin, evaluation of their effects in an ovariectomized rat model is in process.

Abbreviations

DRTF	total Drynariae Rhizoma flavonoids
E_2	17-β-estradiol
ER	estrogen receptor
OPG	osteoprotegrin
RANKL	receptor activator of NF–κB ligand
OVX	ovariectomy
ERT	estrogen replacement therapy
PMOP	postmenopausal osteoporosis
BMC	bone mineral content
BMD	bone mineral density
S-Ca	serum calcium
S-P	serum phosphorus
ALP	alkaline phosphatase
U-Ca	urine calcium
U-P	urine phosphorus
Cr	creatinine
DPD	deoxypyridinoline
CTX-I	C-terminal telopeptide of type I collagen
OC	osteocalcin
PICP	propeptide of type I procollagen
TRAP	tartrate-resistant acid phosphatase
BV/TV	bone volume/tissue volume
Tb.N	trabecular number
Tb.Th	trabecular thickness
Tb.Sp	trabecular separation
Tb.Pf	trabecular pattern factor
Cb.Th	cortical thickness

Author contributions

Shuanghong Song: Performed the in vivo experiment, in vitro experiment, analyzed the data, interpreted results of experiments and prepared the manuscript; Yuankun Zhai: Participated in the animal experiment and revised the manuscript; Qian Yu: Participated in the in vitro experiment; Yuan Zhang, Wenping Hua, Yi Lu: Established the analytical method and reviewed the final manuscript; Peng Shang, Cuiqin Li, Zhezhi Wang: Guidance for planning, execution of experiment and proof reading and manuscript revision. All the authors have read and approved the final version.

Conflicts of interest

The authors declare that there is no conflict of interest regarding the publication of this paper.

Acknowledgments

The authors would like to thank Dr. Hong Zhou (The University of Sydney, Australia) for generously providing MC3T3-E1 cell line. This work benefited from financial support from the TianZhou-1 (TZ-1) Space program of China manned space project, the Northwestern Polytechnical University Foundation for Science and Technology Innovation, the Northwestern Polytechnical University Foundation for

Fundamental Research (Grant No. 3102014ZD0045), the National Natural Science Foundation of China (Grant No. 81501062) and the Fundamental Research Funds for the Central Universities (Grant No. GK201603114).

References

Al-Anazi, A.F., Qureshi, V.F., Javaid, K., Qureshi, S., 2011. Preventive effects of phytoestrogens against postmenopausal osteoporosis as compared to the available therapeutic choices: an overview. J. Nat. Sci. Biol. Med. 2, 154–163.

Banu, J., Varela, E., Fernandes, G., 2012. Alternative therapies for the prevention and treatment of osteoporosis. Nutr. Rev. 70, 22–40.

Bonjour, J.P., Benoit, V., Rousseau, B., Souberbielle, J.C., 2012. Consumption of vitamin D- and calcium-fortified soft white cheese lowers the biochemical marker of bone resorption TRAP 5b in postmenopausal women at moderate risk of osteoporosis fracture. J. Nutr. 142, 698–703.

Boonchird, C., Mahapanichkul, T., Cherdshewasart, W., 2010. Differential binding with ERalpha and ERbeta of the phytoestrogen-rich plant *Pueraria mirifica*. Braz. J. Med. Biol. Res. 43, 195–200.

Bord, S., Ireland, D.C., Beavan, S.R., Compston, J.E., 2003. The effects of estrogen on osteoprotegerin, RANKL, and estrogen receptor expression in human osteoblasts. Bone 32, 136–141.

Bouxsein, M.L., 2003. Mechanisms of osteoporosis therapy: a bone strength perspective. Clin. Cornerstone 2 (Supp l), S13–S21.

Boyce, B.F., Xing, L., 2008. Functions of RANKL/RANK/OPG in bone modeling and remodeling. Arch. Biochem. Biophys. 473, 139–146.

Cassidy, A., 2003. Dietary phytoestrogens and bone health. J. Br. Menopause Soc. 9, 17–21.

Chang, S., Chen, W., Yang, J., 2009. Another formula for calculating the gene change rate in real-time RT-PCR. Mol. Biol. Rep. 36, 2165–2168.

Chen, L.L., Lei, L.H., Ding, P.H., Tang, Q., Wu, Y.M., 2011a. Osteogenic effect of Drynariae rhizoma extracts and Naringin on MC3T3-E1 cells and an induced rat alveolar bone resorption model. Arch. Oral Biol. 56, 1655–1662.

Chen, W.F., Mok, S.K., Wang, X.L., Lai, K.H., Lai, W.P., Luk, H.K., et al., 2011b. Total flavonoid fraction of the *Herba epimedii* extract suppresses urinary calcium excretion and improves bone properties in ovariectomised mice. Br. J. Nutr. 105, 180–189.

Davison, S., Davis, S.R., 2003. Hormone replacement therapy: current controversies. Clin. Endocrinol. 58, 249–261.

Delmas, P.D., Eastell, R., Garnero, P., Seibel, M.J., Stepan, J., 2000. The use of biochemical markers of bone turnover in osteoporosis. Osteoporos. Int. 11 (Suppl 6), S2–17.

Devareddy, L., Khalil, D.A., Smith, B.J., Lucas, E.A., Soung do, Y., Marlow, D.D., et al., 2006. Soy moderately improves microstructural properties without affecting bone mass in an ovariectomized rat model of osteoporosis. Bone 38, 686–693.

Dixon, R.A., 2004. Phytoestrogens. Annu. Rev. Plant Biol. 55, 225–261.

Ederveen, A.G., Spanjers, C.P., Quaijtaal, J.H., Kloosterboer, H.J., 2001. Effect of 16 months of treatment with tibolone on bone mass, turnover, and biomechanical quality in mature ovariectomized rats. J. Bone Miner. Res. 16, 1674–1681.

Ehrlich, L.A., Chung, H.Y., Ghobrial, I., Choi, S.J., Morandi, F., Colla, S., et al., 2005. IL-3 is a potential inhibitor of osteoblast differentiation in multiple myeloma. Blood 106, 1407–1414.

Foidart, J.M., Desreux, J., Pintiaux, A., Gompel, A., 2007. Hormone therapy and breast cancer risk. Climacteric 10 (Suppl 2), 54–61.

Haguenauer, D., Welch, V., Shea, B., Tugwell, P., Adachi, J.D., Wells, G., 2000. Fluoride for the treatment of postmenopausal osteoporotic fractures: a meta-analysis. Osteoporos. Int. 11, 727–738.

Huang, Y., Liu, X., Zhao, L., Li, F., Xiong, Z., 2014. Kidney tissue targeted metabolic profiling of glucocorticoid-induced osteoporosis and the proposed therapeutic effects of Rhizoma Drynariae studied using UHPLC/MS/MS. Biomed. Chromatogr. 28, 878–884.

Hvidtfeldt, U.A., Tjonneland, A., Keiding, N., Lange, T., Andersen, I., Sorensen, T.I., et al., 2015. Risk of breast cancer in relation to combined effects of hormone therapy, body mass index, and alcohol use, by hormone-receptor status. Epidemiology 26, 353–361.

Jeong, J.C., Kang, S.C., Jeong, C.W., Kim, H.M., Lee, Y.C., Chang, Y.C., et al., 2003. Inhibition of Drynariae Rhizoma extracts on bone resorption mediated by processing of cathepsin K in cultured mouse osteoclasts. Int. Immunopharmacol. 3, 1685–1697.

Kuiper, G.G., Lemmen, J.G., Carlsson, B., Corton, J.C., Safe, S.H., van der Saag, P.T., et al., 1998. Interaction of estrogenic chemicals and phytoestrogens with estrogen receptor beta. Endocrinology 139, 4252–4263.

Kyvernitakis, I., Kostev, K., Hars, O., Albert, U.S., Kalder, M., Hadji, P., 2015. Persistency with estrogen replacement therapy among hysterectomized women after the Women's Health Initiative study. Climacteric 18, 826–834.

Laib, A., Barou, O., Vico, L., Lafage-Proust, M.H., Alexandre, C., Rugsegger, P., 2000. 3D micro-computed tomography of trabecular and cortical bone architecture with application to a rat model of immobilisation osteoporosis. Med. Biol. Eng. Comput. 38, 326–332.

Laib, A., Kumer, J.L., Majumdar, S., Lane, N.E., 2001. The temporal changes of trabecular architecture in ovariectomized rats assessed by MicroCT. Osteoporos. Int. 12, 936–941.

Lampe, J.W., 2003. Isoflavonoid and lignan phytoestrogens as dietary biomarkers. J. Nutr. 133 (Suppl 3), 956S–964S.

Lau, W.S., Chan, R.Y., Guo, D.A., Wong, M.S., 2008. Ginsenoside Rg1 exerts estrogen-like activities via ligand-independent activation of ERalpha pathway. J. Steroid Biochem. Mol. Biol. 108, 64–71.

Lu, Y., Zhang, C., Bucheli, P., Wei, D., 2006. Citrus flavonoids in fruit and traditional Chinese medicinal food ingredients in China. Plant Foods Hum. Nutr. 61, 57–65.

Magnusson, C., Weiderpass, E., 2001. Hormone therapy in climacteric. Different effects of estrogen and gestagen on the risk of breast and endometrial cancer. Lakartidningen 98, 418–421.

Marinozzi, F., Bini, F., Marinozzi, A., Zuppante, F., De Paolis, A., Pecci, R., et al., 2013. Technique for bone volume measurement from human femur head samples by classification of micro-CT image histograms. Ann. Ist. Super. Sanita 49, 300–305.

Miura, H., Yamamoto, I., Yuu, I., Kigami, Y., Ohta, T., Yamamura, Y., et al., 1995. Estimation of bone mineral density and bone loss by means of bone metabolic markers in postmenopausal women. Endocr. J. 42, 797–802.

Mok, S.K., Chen, W.F., Lai, W.P., Leung, P.C., Wang, X.L., Yao, X.S., et al., 2010. Icariin protects against bone loss induced by oestrogen deficiency and activates oestrogen receptor-dependent osteoblastic functions in UMR 106 cells. Br. J. Pharmacol. 159, 939–949.

Morch, L.S., Lokkegaard, E., Andreasen, A.H., Kruger-Kjaer, S., Lidegaard, O., 2009. Hormone therapy and ovarian cancer. JAMA 302, 298–305.

Morch, L.S., Lokkegaard, E., Andreasen, A.H., Kjaer, S.K., Lidegaard, O., 2012. Hormone therapy and ovarian borderline tumors: a national cohort study. Cancer Causes Control 23, 113–120.

Muller, R., Hannan, M., Smith, S.Y., Bauss, F., 2004. Intermittent ibandronate preserves bone quality and bone strength in the lumbar spine after 16 months of treatment in the ovariectomized cynomolgus monkey. J. Bone Miner. Res. 19, 1787–1796.

Nakamuta, H., 2004. The ovariectomized animal model of postmenopausal bone loss. Nihon Rinsho. 62 (Suppl 2), 759–763.

National Pharmacopoeia Committee, 2015. Pharmacopoeia of the People's Republic of China. Part 1. Chemical Industry Press, China, p. 256.

NIH, 2011. Guide for the Care and Use of Laboratory Animals. National Academy of Sciences, Washington DC.

Pang, W.-Y., Wang, X.-L., Mok, S.-K., Lai, W.-P., Chow, H.-K., Leung, P.-C., et al., 2010. Naringin improves bone properties in ovariectomized mice and exerts oestrogen-like activities in rat osteoblast-like (UMR-106) cells. Br. J. Pharmacol. 159, 1693–1703.

Pastoureau, P., Chomel, A., Bonnet, J., 1995. Specific evaluation of localized bone mass and bone loss in the rat using dual-energy X-ray absorptiometry subregional analysis. Osteoporos. Int. 5, 143–149.

de la Piedra, C., Traba, M.L., Dominguez Cabrera, C., Sosa Henriquez, M., 1997. New biochemical markers of bone resorption in the study of postmenopausal osteoporosis. Clin. Chim. Acta 265, 225–234.

Sundeep, K., 2010. Update on estrogens and the skeleton. J. Clin. Endocrinol. Metab. 95, 3569–3577.

Theoleyre, S., Wittrant, Y., Tat, S.K., Fortun, Y., Redini, F., Heymann, D., 2004. The molecular triad OPG/RANK/RANKL: involvement in the orchestration of pathophysiological bone remodeling. Cytokine Growth Factor Rev. 15, 457–475.

Turner, C.H., Burr, D.B., 1993. Basic biomechanical measurements of bone: a tutorial. Bone 14, 595–608.

Turner, C.H., Hasegawa, K., Zhang, W., Wilson, M., Li, Y., Dunipace, A.J., 1995. Fluoride reduces bone strength in older rats. J. Dent. Res. 74, 1475–1481.

Wang, X.L., Wang, N.L., Zhang, Y., Gao, H., Pang, W.Y., Wong, M.S., et al., 2008. Effects of eleven flavonoids from the osteoprotective fraction of *Drynaria fortunei* (KUNZE) J. SM. on osteoblastic proliferation using an osteoblast-like cell line. Chem. Pharm. Bull. (Tokyo) 56, 46–51.

Wong, R.W., Rabie, B., Bendeus, M., Hagg, U., 2007. The effects of Rhizoma Curculiginis and Rhizoma Drynariae extracts on bones. Chin. Med. 2, 13.

Wronski, T.J., Dann, L.M., Scott, K.S., Cintron, M., 1989. Long-term effects of ovariectomy and aging on the rat skeleton. Calcif. Tissue Int. 45, 360–366.

Xie, Y.M., Ju, D.H., Zhao, J.N., 2004. Effect of osteopractic total flavone on bone mineral density and bone histomorphometry in ovariectomized rats. Chin. J. Chin. Mater. Med. 29, 343–346.

Xu, T., Wang, L., Tao, Y., Ji, Y., Deng, F., Wu, X.H., 2016. The function of naringin in inducing secretion of osteoprotegerin and inhibiting formation of osteoclasts. Evid. Based Complement. Alternat. Med. 2016, 8981650.

Yang, R.S., Lin, W.L., Chen, Y.Z., Tang, C.H., Huang, T.H., Lu, B.Y., et al., 2005. Regulation by ultrasound treatment on the integrin expression and differentiation of osteoblasts. Bone 36, 276–283.

Zhai, Y.K., Guo, X.Y., Ge, B.F., Zhen, P., Ma, X.N., Zhou, J., et al., 2014. Icariin stimulates the osteogenic differentiation of rat bone marrow stromal cells via activating the PI3K-AKT-eNOS-NO-cGMP-PKG. Bone 66, 189–198.

Zhang, Y., Chen, W.F., Lai, W.P., Wong, M.S., 2008. Soy isoflavones and their bone protective effects. Inflammopharmacology 16, 213–215.

Zhang, Y., Li, Q., Wan, H.Y., Helferich, W.G., Wong, M.S., 2009. Genistein and a soy extract differentially affect three-dimensional bone parameters and bone-specific gene expression in ovariectomized mice. J. Nutr. 139, 2230–2236.

Zhang, Y., Li, Q., Li, X., Wan, H.Y., Wong, M.S., 2010. *Erythrina variegata* extract exerts osteoprotective effects by suppression of the process of bone resorption. Br. J. Nutr. 104, 965–971.

Zhang, Y., Li, Q., Wan, H.Y., Xiao, H.H., Lai, W.P., Yao, X.S., et al., 2011. Study of the mechanisms by which *Sambucus williamsii* HANCE extract exert protective effects against ovariectomy-induced osteoporosis in vivo. Osteoporos. Int. 22, 703–709.

Zhang, R., Pan, Y.L., Hu, S.J., Kong, X.H., Juan, W., Mei, Q.B., 2014a. Effects of total lignans from *Eucommia ulmoides* barks prevent bone loss in vivo and in vitro. J. Ethnopharmacol. 155, 104–112.

Zhang, Z., Song, C., Fu, X., Liu, M., Li, Y., Pan, J., et al., 2014b. High-dose diosgenin reduces bone loss in ovariectomized rats via attenuation of the RANKL/OPG ratio. Int. J. Mol. Sci. 15, 17130–17147.

Zhu, H.F., Wang, W.J., Wang, Z.M., 2010. Effects of Drynariae Rhizoma total flavone on Smad1 Smad5 mRNA expression in osteoporotic rats. Chinese Archives of Traditional Chinese Medicine 28, 200–204.